Electronic transport studies on $Sb_{1-x}(SiO_2)_x$ films

2005 J. Phys.: Condens. Matter 17 2553

(http://iopscience.iop.org/0953-8984/17/17/003)

INSTITUTE OF PHYSICS PUBLISHING JOURNAL OF PHYSICS: CONDENSED MATTER

J. Phys.: Condens. Matter **17** (2005) 2553–2562 doi:10.1088/0953-8984/17/17/003

Electronic transport studies on $Sb_{1-x}(SiO_2)_x$ films

J Du[1,2], Z Q Li[3], J J Lin[3], H Liu[1], R K Zheng[1], P Chen[1], R Rosenbaum[4] and X X Zhang[1,5]

[1] Department of Physics and Institute of Nano Science and Technology, The Hong Kong University of Science and Technology, Clear Water Bay, Kowloon, Hong Kong
[2] National Laboratory of Solid State Microstructures and Department of Physics, Nanjing University, Nanjing 210093, People's Republic of China
[3] Institute of Physics and Department of Electrophysics, National Chiao Tung University, Hsinchu 300, Taiwan
[4] School of Physics and Astronomy, Tel Aviv University, Ramat Aviv, 69978, Israel

E-mail: phxxz@ust.hk

Received 21 February 2005, in final form 30 March 2005
Published 15 April 2005
Online at stacks.iop.org/JPhysCM/17/2553

Abstract

$Sb_{1-x}(SiO_2)_x$ granular films were prepared by the co-sputtering method with the volume fraction of SiO_2, x, ranging from 0 (i.e. pure Sb) to about 30%. Systematic electronic transport studies, including resistivity, magnetoresistance, Hall effect and Seebeck effect, were carried out against the temperature, magnetic field and volume fraction x of SiO_2. With the gradual increase of the SiO_2 content, the mean grain size of the Sb decreases, and eventually the film becomes amorphous, as illustrated by the changes of the x-ray diffraction patterns. The temperature coefficient of resistivity also changes its sign from positive to negative, indicating a semimetal–semiconductor or insulator transition. Magnetoresistance studies using the weak localization theory revealed that the electron dephasing time follows approximately a T^{-2} law. This behaviour indicates that the electron–phonon (e–ph) scattering still dominates the electron dephasing processes in these granular systems with a fair number of SiO_2 inclusions. The Hall coefficient decreases monotonically with temperature and with the volume fraction of SiO_2. The giant Hall effect is absent in these granular films. Finally, an interesting but rather complicated behaviour of the Seebeck coefficient versus temperature was observed when the volume content of the SiO_2 exceeded 18%.

1. Introduction

The transport properties of metal–insulator granular films have attracted much interest in the past several decades. The Hall effect essentially reflects the density and the sign of the charge

[5] Author to whom any correspondence should be addressed.

carriers. In the past several years, a significantly enhanced Hall effect, i.e., the giant Hall effect (GHE), was found in both magnetic [1, 2] and non-magnetic [3] granular systems, such as magnetic NiFe–SiO_2 and non-magnetic Cu–SiO_2 films. Although these effects cannot be explained by the conventional percolation model [4], they can be well accounted for by a new mechanism based on the local quantum interference effect [5]. Within this theoretical framework, it is argued that a *large* electron dephasing length [5] in the small substructures is the most important factor resulting in the giant Hall effect. To our knowledge, a semimetal like antimony (Sb) has a large mean free path [6] and an electron dephasing length [7] of more than 2000 Å at 5 K. Few people have studied the Hall effect and other transport properties in the granular antimony films.

Recently, the search for high quality thermoelectric (TE) materials by using low dimensional systems has become an active research field [8]. The TE efficiency is usually expressed by a dimensionless figure of merit: $Z_{\mathrm{TE}} = S^2T/\rho\kappa$, where S, ρ, κ and T are the Seebeck coefficient (or thermopower), electrical resistivity, thermal conductivity and absolute temperature, respectively. In order to enhance the figure of merit, theoretical works have predicted that this could be accomplished by introducing the inclusion of particles of a few nanometres in a polycrystalline material [9, 10]. The nano-inclusions must be insulating [11], chemically stable and inert with regard to the matrix [12]. It is well known that the group V semimetal bismuth (Bi) and its related alloys are promising candidates for low dimensional TE materials at ∼100 K [13]. Therefore, Brochin *et al* [14] have tried to make bismuth–silica (Bi–SiO_2) nanocomposites; however, no significant improvement of the thermoelectric property was observed compared to bulk Bi.

In this work, we study Sb–SiO_2 granular films. For bulk semimetal antimony (Sb), its electronic transport is also governed via both electrons and holes as in Bi. The energy overlap between the conduction and valence bands is about 180 meV at 4.2 K [15], which is much larger than that of Bi. However, when Sb is prepared in the form of a thin film, the two bands will split apart and a bandgap will be created if the thickness is quite small; this phenomenon is known as the quantum size effect [16, 17]. Similarly, when SiO_2 is introduced into an Sb film, it will inhibit the growth of the Sb grains. Consequently, the band structure of the Sb will be *modified* in a similar manner, resulting in the change of the transport properties. In this work, polycrystalline Sb and a series of Sb–SiO_2 granular films have been fabricated, and their electronic transport properties have been measured as a function of temperature and volume fraction x of SiO_2.

2. Experimental method

$Sb_{1-x}(SiO_2)_x$ granular films with different SiO_2 volume fractions were fabricated by using the co-sputtering technique on glass or Kapton substrates at ambient temperature. The base pressure was below 2×10^{-7} Torr and the Ar pressure was 4×10^{-3} Torr during deposition. By adjusting the powers of the Sb and SiO_2 targets, different compositions could be achieved. The SiO_2 atomic ratios for all the films were obtained from x-ray fluorescence (XRF), and the volume fraction x could be calculated consequently. In our films, x varies from 0 (pure Sb) to about 30%; the thicknesses for all the films were kept to about 0.45 μm. The dc resistance was measured by a standard four-probe technique, and the Hall effect was measured by the five-contact method. The temperature dependences of the resistance and magnetoresistance were measured using a Quantum Design physical property measurement system (PPMS). The Seebeck coefficient was measured using a home built sample probe as described previously [18].

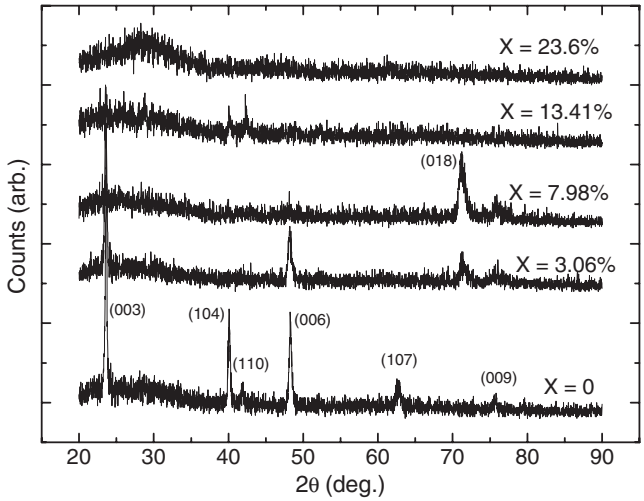

Figure 1. X-ray diffraction patterns of an Sb film ($x = 0$) and $Sb_{1-x}(SiO_2)_x$ granular films with $x = 3.06\%$, 7.98%, 13.41% and 23.6%.

3. Results and discussion

3.1. X-ray diffraction

Figure 1 shows the x-ray diffraction patterns of pure Sb and some representative Sb–SiO_2 films. It is clearly seen that the as-deposited pure Sb film is polycrystalline with the (003) plane as the preferred orientation rather than the (102) plane of the powder form [19]. As the content of the SiO_2 inclusions increases, the diffraction peaks become weaker and broader, and eventually no obvious peaks can be detected when the volume fraction of SiO_2, x, is higher than 13.41%, indicating an appearance of an *amorphous* structure.

The average grain size, d, can be determined from the diffraction peaks by using the expression [20]

$$d = \lambda/(B_c \cos\theta) \tag{1}$$

where λ is the x-ray wavelength, θ is the Bragg angle and B_c is the true width of the diffraction peak at half of the maximum intensity. For example, for the pure Sb film ($x = 0$) and the Sb–SiO_2 films with $x = 3.06\%$ and 13.41%, d is estimated to be about 40, 32 and 20 nm, respectively.

3.2. Resistance ratios and resistivity

The normalized resistance, $R(T)/R$ (300 K), versus temperature has been displayed in figure 2. For the pure Sb film, the resistance increases slowly with increasing T, exhibiting a metallic behaviour with a positive temperature coefficient of resistivity (TCR). However, as x increases the temperature dependence of the normalized resistance becomes weaker and weaker. When x is larger than 13.41% the TCR becomes negative, and if x is increased further the normalized resistance becomes more and more strongly temperature dependent. For example, for the sample having $x = 23.60\%$ (not shown here), it decreases by about three orders of magnitude when the temperature varies from 5 to 300 K. This behaviour indicates a typical insulator behaviour. Figure 3 shows the room temperature resistivity ρ as a function of the volume

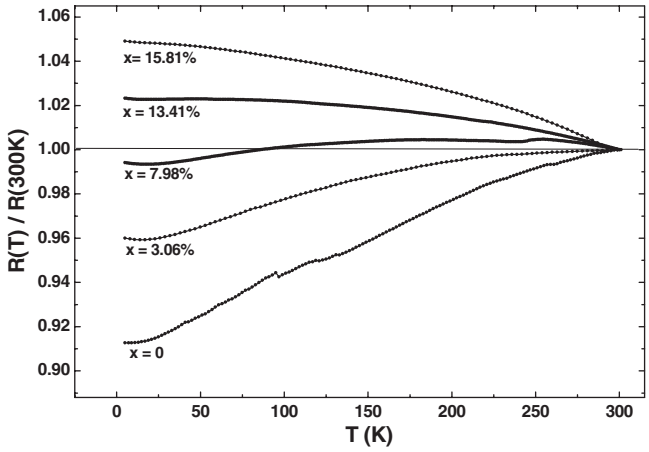

Figure 2. Temperature dependence of the normalized resistance, $R(T)/R$ (300 K), of the samples with $x = 0$, 0.306%, 7.98%, 13.41% and 15.81%.

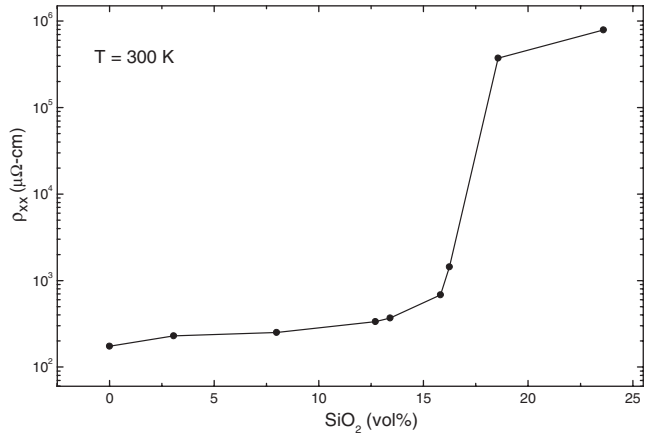

Figure 3. The resistivity versus the volume fraction x of SiO_2 at $T = 300$ K.

fraction x of SiO_2. The resistivity increases slowly when x is lower than 15%. However, when x changes from 15% to 18%, there is a significant increase of about three orders of magnitude for the resistivity; there is a structural change from polycrystalline to amorphous states.

The resistance ratio behaviours in figure 2 are complicated to explain. For the films having low SiO_2 content, the decreasing resistances with decreasing temperature most likely result from the freezing out of phonons and hence weaker scattering within the Sb grains; this results in increasing larger values of the mobilities and decreasing resistances. For larger SiO_2 content, there is stronger boundary scattering of the carriers at the numerous SiO_2 boundaries, a temperature independent scattering process. This results in a competition between the phonon and boundary scattering processes; thus the resistance changes little with temperature. Moreover, for the samples having the highest SiO_2 content of 13.41% and 15.81%, the temperature independent boundary scattering term dominates. But there is also a small decrease of both the number of holes and electrons with decreasing temperature, which causes the resistance to slowly rise with lowering temperature.

3.3. Magnetoresistance results

The electron dephasing scattering time, τ_φ, is a quantity of fundamental interest and importance in disordered metals and mesoscopic systems [21]. The dephasing scattering time can be extracted from the magnetoresistance (MR) data using the three-dimensional (3D) weak localization (WL) theory, provided that the sample is *metallic*. Here MR $= [R(B) - R(0)]/R(0)$. In 3D weakly disordered metals, the electron–phonon (e–ph) scattering is the dominant inelastic dephasing process, and τ_φ is given by [21]

$$\tau_\varphi^{-1}(T) = \tau_c^{-1} + \tau_{ep}^{-1}(T) = \tau_c^{-1} + AT^p, \tag{2}$$

where τ_c is a constant (the zero-temperature dephasing time), whose origin is currently under much debate; τ_{ep} is the electron–phonon scattering time, A is the strength of the e–ph interaction, and usually $2 \leqslant p \leqslant 4$ in three dimensions. According to the theory of Rammer and Schmid [23], the e–ph scattering rate $1/\tau_{ep}$ is proportional to T^3 ($p = 3$) in the pure metals and T^4 ($p = 4$) in the dirty limit $ql \ll 1$, where q is the wavenumber of the thermal phonons and l is the electron elastic mean free path. However, in the literature [21, 24], it has been found in many materials that $1/\tau_{ep} \sim T^2$ ($p \sim 2$). Recently, this T^2 behaviour in the dirty limit has been theoretically addressed by Sergeev and Mitin [25]. It also becomes clear that the T^4 law is absent in most measurements because the materials studied may contain 'static' defects which do not vibrate with the deformed lattice atoms [26, 27].

We have previously studied several thick Sb films having intermediate levels of disorder ($ql \sim 1$) and obtained the effective exponent of temperature $p \approx 2.4 \pm 0.2$ [22]. In this present study with increasing the inclusions of SiO_2, it is reasonable for us to speculate that the granular system becomes more and more disordered compared with the pure Sb film. Therefore, it will be very interesting to know how the p value changes.

Using the magnetoconductivity (MC) data measured in low magnetic fields as shown in figure 4 and fitting the MC data using the 3D weak-localization expressions summarized in [28], we extracted values of τ_{ep} and then the p values (or, equivalently, the electron dephasing length $L_\varphi = (D\tau_{ep})^{1/2}$, where D is the diffusion constant). In figure 4, the magnetoresistivities are positive, because the spin–orbit scattering is strong in the sample due to the presence of heavy Sb atoms. At low fields, the weak localization theory can describe well the experimental data. At high fields, small deviations are expected because the electron–electron interactions and other effects might no longer be negligible.

For the present discussion, two representative samples with the SiO_2 components of 13.41% and 15.81% were chosen. Their dependences of the fitted $L_\varphi = (\tau_{ep}D)^{1/2}$ (solid and open circles) versus temperature are shown in figure 5. The value used for D is 6.2×10^{-4} m^2 s^{-1} for the $x = 15.81\%$ sample and $D = 11.4 \times 10^{-4}$ m^2 s^{-1} for the $x = 13.41\%$ sample. The extracted τ_{ep} values yielded $p \approx 2$ and ≈ 2.4 for $x = 13.41\%$ and 15.81%, respectively. These results reveal that the e–ph scattering is still the dominating inelastic dephasing process, even by introducing an appropriate amount of SiO_2 inclusions into the Sb semimetal to make it more disordered. Moreover, inspection of the measured magnitudes of L_φ shown in figure 5 justifies our use of the 3D weak-localization theoretical predictions to describe our MR results, i.e., L_φ is much smaller than the thickness (0.45 μm) of our films. From figure 5, the magnitudes of the dephasing lengths are of the same order of magnitude as the diameters of the Sb grains, and hence one would not anticipate observing the giant Hall effect in this material.

3.4. Hall voltage measurements

Since theory predicts that a *large* electron dephasing length L_φ is directly associated with the giant Hall effect observed in the non-magnetic *granular* Cu–SiO_2 film system [5], it is of great

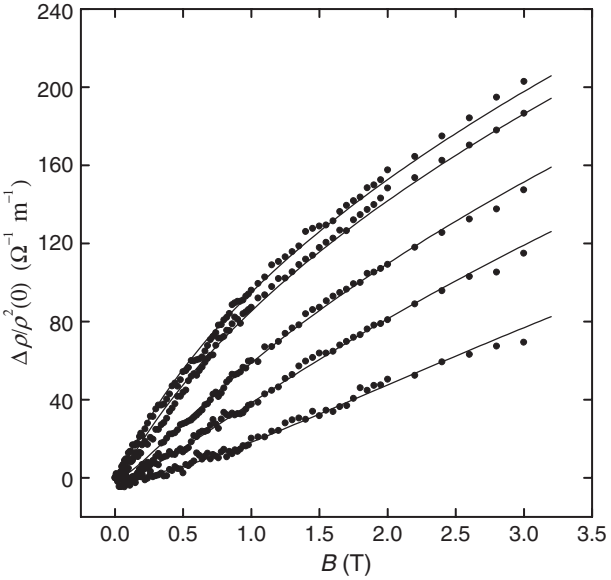

Figure 4. The normalized magnetoresistivities, $\Delta\rho/\rho^2(0) = [\rho(B) - \rho(0)]/\rho^2(0)$, as a function of magnetic field for the film with $x = 13.4\%$ at 4.0, 5.0, 7.0, 10.0 and 15.0 K from top to bottom. The symbols are the experimental data and the solid curves are the least-squares fits using the 3D weak-localization theoretical predictions.

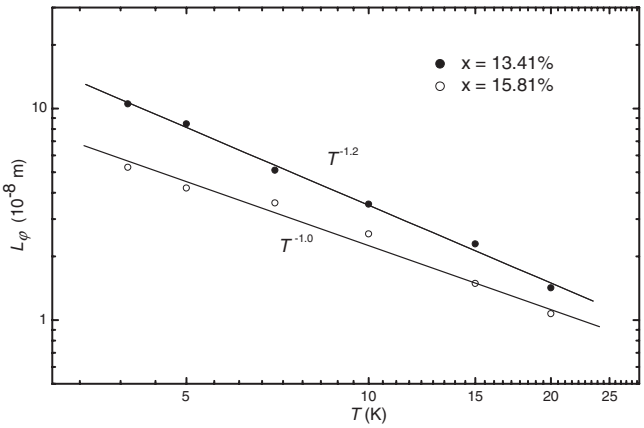

Figure 5. Temperature dependence of the electron dephasing length, L_φ, of samples with $x = 13.41\%$ and 15.81%. The solid lines are least-squares fits using equation (2).

interest to carry out Hall voltage measurements V_H on the Sb–SiO_2 films. Values for the Hall coefficient R_H are found using the applied measuring current I and magnetic field B and the film thickness t, $R_H = tV_H/IB$.

Figure 6(a) shows the Hall coefficient R_H versus temperature for several Sb–SiO_2 samples with $x \leqslant 15.81\%$. For clarity, the dependence of R_H measured at room temperature on the SiO_2 volume fraction is shown in figure 6(b). R_H decreases monotonically with increasing temperature and with the content of the SiO_2. Oktu and Saunders [29] have systematically studied the Hall effect in the temperature range between 77 and 273 K in single-crystal antimony. Their results also show that the Hall coefficient decreases monotonically with

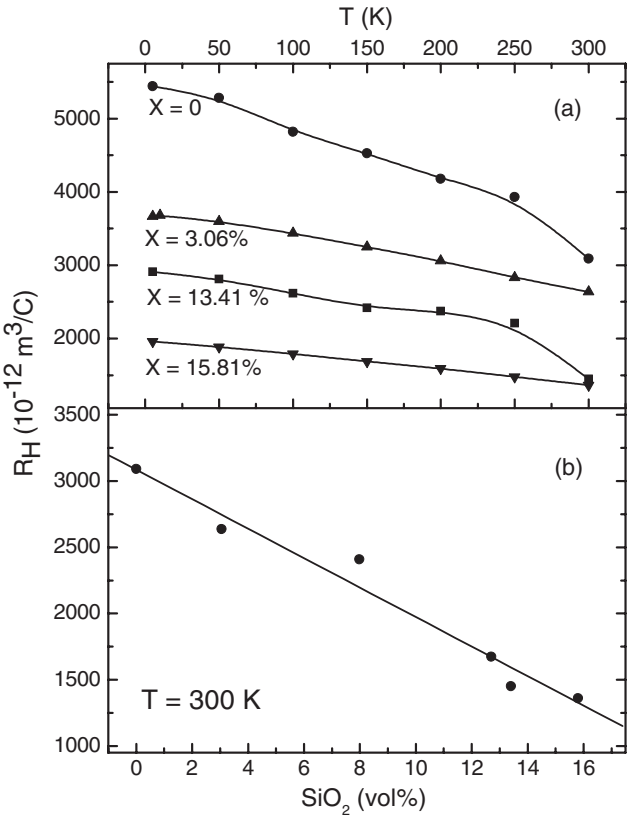

Figure 6. (a) Temperature dependences of the Hall coefficients R_H of the samples with $x = 0$, 3.06%, 13.41% and 15.81%; (b) the Hall coefficients versus the volume fraction x of SiO_2 at $T = 300$ K.

increasing temperature; and the ratio of R_H between 77 and 273 K is about 1.78, which is close to that of our polycrystalline Sb film within the same temperature range.

If x is larger than 15.81%, no accurate Hall voltage values could be measured owing to their *small* magnitudes and owing to temperature fluctuations that caused large resistance variations in these insulating films. We speculate that no giant Hall effect should be observed in these samples, owing to the amorphous structure of the Sb; that is, there are no longer crystalline grains of Sb. For this reason, the theory of Wan and Sheng [5], which considers conductor–dielectric nanocomposites having a well defined percolation threshold of the conductor volume faction, does not apply.

For pure antimony, the Hall coefficient in the low field limit should be given by the following expression which holds for a material having both electron and hole carriers [30–32]:

$$R_H \approx (-1/|e|)[n_e\mu_e^2 - n_h\mu_h^2]/[(n_e\mu_e + n_h\mu_h)^2], \tag{3}$$

where $|e|$ is the magnitude of the electronic charge, n_h and n_e are the densities of holes and electrons respectively, and μ_h and μ_e are their mobilities. Equation (3) can be simplified as

$$R_H \approx (1/n|e|)[(b-1)/(b+1)]; \tag{4}$$

here $b = \mu_h/\mu_e$. For Sb assuming $n_h = n_e = n$, the measured Hall voltage is always positive implying that $\mu_h > \mu_e$. So the Hall coefficient is essentially determined by the carrier density and the ratio between the hole mobility and the electron mobility.

The decrease of R_H in our films might be understood by the following arguments. Although the carrier densities are almost temperature independent, they still increase from 3.9×10^{19} cm^{-3} at 77 K to 4.2×10^{19} cm^{-3} at 273 K for both electrons and holes, resulting in a slight decrease of R_H with increasing temperature. Secondly, although μ_h and μ_e both decrease with increasing temperature following an approximately $T^{-3/2}$ dependence [29], there is still a subtle asymmetry between them, which causes b and hence R_H to decrease.

3.5. Seebeck coefficient

The Seebeck effect has a strong relationship with the transport properties of materials. Figures 7(a) and (b) display the Seebeck coefficient, S, versus temperature for the Sb–SiO_2 samples with x varying from 0 (pure Sb) to 28.86%. For $x \leqslant 18.41\%$, S is positive and increases almost linearly with increasing temperature, shown in figure 7(a). The positive sign reflects the higher mobilities of the holes compared to those of the electrons, which is consistent with the positive Hall coefficients. For all these metallic samples, the curves do not differ too much. The S values are quite small and are not greater than 20 μV K^{-1} even at 300 K; this value is similar to that of vacuum deposited antimony films [33]. In the vacuum deposited films, the linear T dependence could also be observed and explained using the free carrier theory, if the carriers are degenerate ($k_B T \ll E_F$). Therefore, in the present metallic Sb–SiO_2 films, the similar T behaviours of S also confirm that the carriers are still degenerate. In addition, it was claimed that in the case of small volume fractions of insulating inclusions, the Seebeck coefficient is not sensitive to that of inclusions [34, 35], which could probably explain why the Seebeck results do not change too much for $x \leqslant 18.41\%$. Some small variations between the curves would be anticipated, which may be due to the fact that the crystalline structure and the band structure of Sb have been modified due to the SiO_2 inclusions.

However when x is increased above 18.41%, the temperature dependences of the Seebeck coefficient change significantly as illustrated in figure 7(b). The S curves for three different samples ($x = 21.28\%$, 23.60% and 28.86%) behave quite similarly and almost merge together. At room temperature S is negative, as opposed to those of samples with lower SiO_2, suggesting that the mobility of the electrons becomes larger than that of the holes. And its absolute value can approach approximately 200 μV K^{-1}, which is comparable to that of conventional thermoelectric materials. As the temperature decreases, S decreases and changes its sign from negative to positive at around 230 K, as clearly displayed in the inset of figure 7(b). After a non-monotonic variation, S changes its sign back to negative at around 95 K. Then its absolute value increases sharply as the temperature keeps decreasing, behaving like an insulator. This complicated Seebeck behaviour looks quite interesting and has never been observed in other insulating granular systems. This behaviour is most likely correlated with the complicated band structure resulting from the inclusions of the SiO_2. Although S can reach about 200 μV K^{-1} at room temperature, the thermoelectric efficiency described by the figure of merit is small due to the extremely large resistivity. Finally, the absolute values of Seebeck coefficient versus the SiO_2 volume ratio x at temperatures 300 and 50 K are clearly shown in figure 7(c). These results reveal sharp increases after x exceeds 18%, where the metal–insulator transition takes place. This is consistent with the abrupt change of the resistivity at a similar value of the volume ratio x of SiO_2.

4. Summary

Polycrystalline Sb films and $Sb_{1-x}(SiO_2)_x$ thin films have been fabricated by co-sputtering. Their electronic transport properties have been studied. X-ray diffraction patterns reveal

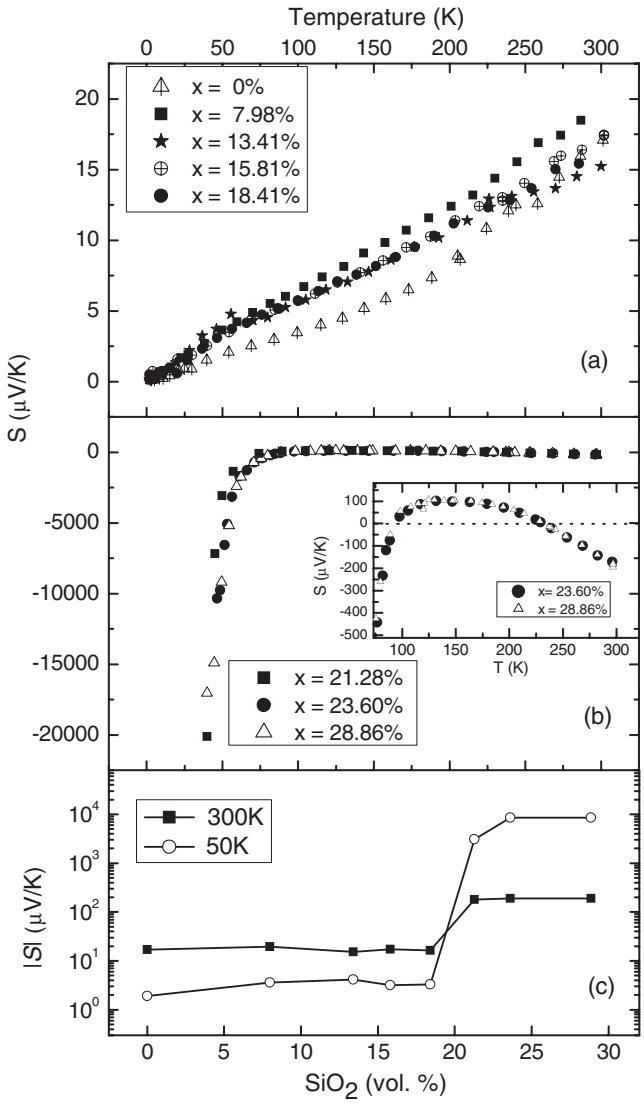

Figure 7. Temperature dependence of the Seebeck coefficient S of different samples: (a) $x = 0$, 7.98%, 13.41%, 15.81% and 18.41%; (b) $x = 21.28\%$, 23.60% and 28.86%. The inset of (b) displays the complicated variation of the Seebeck coefficient of the insulating samples having $x = 23.60\%$ and 28.86%. (c) The absolute values of Seebeck coefficient versus the SiO_2 volume ratio x at temperatures 300 and 50 K. These results reveal sharp increases when x exceeds 18%.

that a structural change from the polycrystalline to the amorphous state happens when the volume fraction of SiO_2, x, increases above 15%. The TCR changes its sign from positive to negative, indicating a semimetal–insulator transition. Magnetoresistance studies indicate that the electron–phonon scattering mechanism dominates the electron dephasing process when $x < 18\%$. The Hall coefficient decreases monotonically with increasing temperature and increasing volume ratio of SiO_2. A complicated behaviour of the Seebeck coefficient was observed when the content of the SiO_2 was larger than 18%.

Acknowledgments

This work is supported by the Hong Kong RGC, grant No 605704. JJL was supported by the Taiwan National Science Council through grant No NSC 93-2112-M-009-009. JD would like to thank the State Key Project of Fundamental Research Grants (No 001CB610602) of China and the National Natural Science Foundation of China (No 10474038) for partial support.

References

[1] Jing X N *et al* 1996 *Phys. Rev.* B **53** 14032
[2] Pakhonov A B, Yan X and Zhao B 1995 *Appl. Phys. Lett.* **67** 3497
[3] Zhang X X, Wan C, Liu H, Li Z Q and Sheng P 2001 *Phys. Rev. Lett.* **86** 5562
[4] Bergman D J and Stroud D 1992 *Solid State Phys.* **46** 149
[5] Wan C and Sheng P 2002 *Phys. Rev.* B **66** 075309
[6] Xu J H and Ting C S 1993 *Appl. Phys. Lett.* **63** 129
[7] Liu J, Meisenheimer T L and Giordana N 1989 *Phys. Rev.* B **40** 7527
[8] Lin Y, Rabin O, Cronin S B, Ying J Y and Dresselhaus M S 2002 *Appl. Phys. Lett.* **81** 2403 and references within
[9] Slack G A and Hussain M A 1991 *J. Appl. Phys.* **70** 2694
[10] Klemens P G 1991 *Mater. Res. Soc. Symp. Proc.* **234** 87
[11] Fluerial J P 1994 *Proc. 12th Int. Conf. on Thermoelectrics (Yokohama, Japan)* ed K Matsuura, p 1
[12] Scoville N *et al* 1995 *Nanostruct. Mater.* **5** 207
[13] Lin Y-M, Sun X and Dresselhaus M S 2000 *Phys. Rev.* B **62** 4610
Sun X, Zhang Z and Dresselhaus M S 1999 *Appl. Phys. Lett.* **74** 4005
[14] Brochin F, Lenoir B, Devaux X, Martin-Lopez R and Scherrer H 2000 *J. Appl. Phys.* **88** 3269
[15] Windmiller L R 1996 *Phys. Rev.* **149** 472
[16] Garcia N, Kao Y K and Strongin M 1972 *Phys. Rev.* B **5** 2029
[17] Hoffman R A and Frankl D R 1971 *Phys. Rev.* B **3** 1825
[18] Li Z Q and Lin J J 2004 *J. Appl. Phys.* **96** 5918
[19] Elfalaky A 1995 *Appl. Phys.* A **60** 87
[20] Jumar A and Katyal O P 1989 *J. Mater. Sci.* **24** 4037
[21] Lin J J and Bird J P 2002 *J. Phys.: Condens. Matter* **14** R501
[22] Lin J J, Li T and Wu T M 2000 *Phys. Rev.* B **61** 3170
[23] Rammer J and Schmid A 1986 *Phys. Rev.* **34** 1352
[24] Lin J J 2000 *Physica* B **279** 191
[25] Sergeev A and Mitin V 2000 *Phys. Rev.* B **61** 6041
Sergeev A and Mitin V 2000 *Europhys. Lett.* **51** 641
[26] Kivinen P, Savin A, Zgirski M, Torma P, Pekola J, Prunnila M and Ahopelto J 2003 *J. Appl. Phys.* **94** 3201
[27] Massilta I J, Karvonen J T, Kivioja J M and Taskinen L J 2003 *Preprint* cond-mat/0311031
[28] Wu C Y and Lin J J 1994 *Phys. Rev.* B **50** 385
[29] Oktu O and Saunders G A 1967 *Phys. Soc.* **91** 156
[30] Leverton W F and Dekker A J 1950 *Phys. Rev.* **80** 732
[31] Fawcett E 1964 *Adv. Phys.* **13** 139
[32] Pippard A B 1989 *Magnetoresistance in Metals* (Cambridge: Cambridge University Press) p 29
[33] Damodara Das V and Soundararajan N 1989 *J. Mater. Sci.* **24** 4315
[34] Bergman D J and Levy O 1991 *J. Appl. Phys.* **70** 6821
[35] Bergman D J and Levy O 1992 *J. Phys. A: Math. Gen.* **25** 1875